ACCOUNTING FOR WALL-INDUCED REYNOLDS STRESS ANISOTROPY IN EXPLICIT ALGEBRAIC STRESS MODELS

Rémi Manceau
Laboratoire d'études aérodynamiques
CNRS UMR 6609, Université de Poitiers
SP2MI, Téléport 2, Bd Marie et Pierre Curie, BP 30179
86 962 Futuroscope Chasseneuil cedex, France
remi.manceau@lea.univ-poitiers.fr

ABSTRACT

The paper is devoted to the derivation of an Explicit Algebraic Stress Model sensitized to the nonlocal blocking effect of the wall through elliptic relaxation. The model is based on the Elliptic Blending Model (Manceau and Hanjalić, 2002), which is projected on a three-term tensorial basis, leading to a three equation transport model (k–ε–α), where α is the elliptic blending function. The model is able to reproduce the two-component limit of turbulence and, in particular, the crucial limiting value of the wall-normal anisotropy $b_{22} = -\frac{1}{3}$ at the wall. The model is shown to perform very well in channel flows at different Reynolds numbers. A comparison with the full Reynolds stress model with elliptic relaxation (13 differential equations) highlights the interest of the approach.

INTRODUCTION

The recent development of Reynolds stress modelling valid down to solid boundaries has led to models able to reproduce the crucial two-component limit of turbulence in the near-wall region without wall or damping functions: however, the degree of complexity of these models, due to highly nonlinear terms (Craft and Launder, 1996) or additional equations (Durbin, 1993), prevents the spreading of these models into industrial codes.

The purpose of the present work is to derive a model as simple as possible while keeping a realistic representation of the physics, and, in particular, of the wall-blocking effect. The method consists in starting from a model with firm theoretical foundations, the SSG Reynolds stress model (Speziale *et al.*, 1991), extended to near-wall regions via the elliptic relaxation strategy (Durbin, 1993) and using inherent properties of the model and mathematical methods in order to reduce the number of equations with a minimum number of hypotheses.

In a first step (Manceau and Hanjalić, 2002), the full model, which contains 13 equations (6 transport equations for the Reynolds stresses, 1 transport equation for the dissipation rate and 6 elliptic relaxation equations accounting for the wall-blocking effect) was reduced to a 8–equation model, the *Elliptic Blending Model.* Indeed, the 6 elliptic relaxation equations of Durbin's model are exactly of the same form and produce the same relaxation effect, linked to the geometry of the domain, on each of the Reynolds stresses: the selective blocking effect is only imposed via different boundary conditions. In the Elliptic Blending Model, the same effect is produced by a single elliptic relaxation equation for a geometrical blending function α, which enables a transition from the standard SSG model far from the wall to a near-wall redistribution model: the model distinguishes among the different Reynolds stress components through the gradient of the blending function α. The Elliptic Blending Model preserves the good properties of the full model (non-locality, near-wall anisotropy representation), and was successfully applied to shear (Manceau and Hanjalić, 2002) and impinging flows (Thielen *et al.*, 2001).

The present work is a further attempt to reach the lowest possible degree of complexity while preserving the physics: the well-known tensor representation theory is used to derive an Explicit Algebraic Stress Model (EASM) (Pope, 1975). The method and the notation follow the paper of Rumsey *et al.* (2000). This results in a model that only consists of 3 transport equations (k–ε–α), but resolves the Reynolds stress anisotropy in all the domain, including the near-wall region.

BACKGROUND MODEL

The Elliptic Blending Model (EBM), described in Manceau and Hanjalić (2002), is derived in order to contain as much physics as possible: it is, similarly to the SSG model, linear with respect to the mean velocity gradient, quadratic with respect to the anisotropy tensor b_{ij}, and depends on the invariants of b_{ij} through:

- the coefficient $(g_3 - g_3^* \sqrt{b_{kl} b_{kl}})$ in front of the term kS_{ij}
- the blending function $Ak\alpha$ used for the dissipation tensor, where A is Lumley's flatness parameter.

In the frame of Explicit Algebraic modelling, it is much easier to work with a fully linear model. Therefore, a slightly different version of the EBM is used here.

- Firstly, the tensorial nonlinear term is simply suppressed by choosing $g_2 = 0$: this term, although necessary to reproduce the return to isotropy problem, is of minor importance in general situations.
- Secondly, the blending functions used to impose a transition to near-wall forms of the redistribution (ϕ_{ij}) and dissipation (ε_{ij}) tensors are both taken as α^2, instead of $k\alpha$ and $Ak\alpha$, respectively. The elliptic relaxation equation then reduces to:

$$\alpha - L^2 \nabla^2 \alpha = 1 \qquad (1)$$

This modification has the virtue of suppressing the numerical instability due to the nonlinearity of the flatness parameter A and the tendency of the blending functions to go to values different from 1 far from the wall.

- Thirdly, the term $(g_3 - g_3^* \sqrt{b_{kl} b_{kl}})\, k S_{ij}$ requires a special treatment. Indeed, it plays a significant role in the near-wall region via the sharp increase of $\sqrt{b_{kl} b_{kl}}$. The same behaviour can be reproduced by using $\sqrt{1-\alpha^2}$ in lieu of $\sqrt{b_{kl} b_{kl}}$. However, this modification is not consistent with rapid distortion theory, which requires this coefficient to go to $g_3 = \frac{4}{5}$ in the limit of initially isotropic turbulence subjected to rapid distortion. Therefore, the term $(g_3 - g_3^* \sqrt{b_{kl} b_{kl}}) k S_{ij}$ is kept unchanged in the version of the EBM used for comparison in the present paper, but replaced by $(g_3 - g_3^* \sqrt{1-\alpha^2})$ in the derivation of the Explicit Algebraic Model: the latter model will not be able to reproduce rapid distortion, but it is anyway the case because of the hypothesis $\partial b_{ij}/\partial t = 0$. Note that in Rumsey *et al.* (2000) model, this term was simply suppressed ($g_3^* = 0$).

The only remaining nonlinearity in the model comes from the term $g_1^* P b_{ij}$, since $P = -2 b_{kl} S_{kl} k$, but this term is kept unchanged, for two reasons: firstly, it is crucial to sensitize the model to departures from the equilibrium value $P/\varepsilon = 1$, and, above all, this nonlinearity cannot be avoided in the Explicit Algebraic methodology, since the product $\tau_{ij} P$ enters the anisotropy transport equation (see Eq. 3). The present, linearized version of the EBM is given extensively in the Appendix.

DERIVATION OF THE EXPLICIT ALGEBRAIC STRESS MODEL

The algebraic methodology (Rodi, 1976), consists in using the equilibrium hypothesis $Db_{ij}/Dt = 0$ and in considering that the anisotropy of the diffusion tensor D_{ij} is the same as that of the Reynolds stress tensor τ_{ij}:

$$\frac{D_{ij}}{D_{kk}} = \frac{\tau_{ij}}{\tau_{kk}} \qquad (2)$$

leading to the algebraic relation:

$$\left(P_{ij} - \frac{\tau_{ij}}{k} P\right) + \phi_{ij} - \left(\varepsilon_{ij} - \frac{\tau_{ij}}{k}\varepsilon\right) = 0 \qquad (3)$$

In order to simplify the equations, a notation similar to the one used by Rumsey *et al.* (2000) is introduced:

$$\begin{aligned}
a_1 &= \frac{2}{3} - \frac{1}{2}\left(g_3 - g_3^* \sqrt{1-\alpha^2}\right)\alpha^2 \\
a_2 &= 1 - \frac{g_5}{2}\alpha^2 \\
a_3 &= 1 - \frac{g_4}{2}\alpha^2 \\
a_4 &= g\mathcal{T} \\
a_5 &= \frac{5}{\mathcal{T}}(1-\alpha^2) \\
\mathcal{T} &= \frac{k}{\varepsilon} \\
g &= \left[\left(1 + \frac{g_1^*}{2}\alpha^2\right)\frac{P}{\varepsilon} - \left(\frac{13}{3} - \frac{g_1}{2}\right)\alpha^2 + \frac{10}{3}\right]^{-1}
\end{aligned} \qquad (4)$$

In Rumsey *et al.* (2000), only a_4 was not a constant, while in Eq. (4), all the coefficients depend on α, which goes from zero at the wall to one far from the wall. This (implicit) dependence on the distance to the wall is at the origin of the transition from the standard SSG model (recovered asymptotically when $\alpha \to 1$) to the near-wall model ($\alpha \to 0$), accounting for the wall-blocking effect.

The EBM involves the vector $\boldsymbol{n}$ defined as $\boldsymbol{n} = \nabla\alpha / \|\nabla\alpha\|$. Since the wall is the isosurface $\alpha = 0$, $\boldsymbol{n}$ gives the wall-normal direction at the wall, but is also well defined in the remaining of the domain. It is convenient to introduce the "wall-normal tensor" $\boldsymbol{N}$ defined by $N_{ij} = n_i n_j$ and its deviatoric part $\boldsymbol{M} = \boldsymbol{N} - \frac{1}{3}\boldsymbol{I}$, where $\boldsymbol{I}$ is the identity tensor. The trace of a tensor $\boldsymbol{A}$ is denoted by $\{\boldsymbol{A}\}$. $\boldsymbol{S}$ and $\boldsymbol{W}$ are the mean strain rate and mean rotation rate tensors, respectively.

Introducing the EBM in Eq. (3) yields:

$$\begin{aligned}
&-\frac{1}{a_4}\boldsymbol{b} - a_3\left(\boldsymbol{bS} + \boldsymbol{Sb} - \frac{2}{3}\{\boldsymbol{bS}\}\boldsymbol{I}\right) \\
&+a_2(\boldsymbol{bW} - \boldsymbol{Wb}) \\
&-a_5\left(\boldsymbol{bM} + \boldsymbol{Mb} - \frac{2}{3}\{\boldsymbol{bM}\}\boldsymbol{I} - \frac{1}{2}\{\boldsymbol{bM}\}\boldsymbol{M}\right) \\
&= a_1\boldsymbol{S} + \frac{a_5}{2}\boldsymbol{M}
\end{aligned} \qquad (5)$$

Again, the wall-blocking effect enters Eq. (5) when $\alpha < 1$, through the variations of the coefficients, in particular by activating the terms in a_5 that involve the wall-normal tensor $\boldsymbol{M}$. Equation (5) reduces to the algebraic form of the SSG model (see, e.g., Rumsey *et al.*, 2000) when $\alpha = 1$.

In order to find an explicit solution of Eq. (5), a Galerkin projection is used. It is easy to show that in two-dimensional flows, the anisotropy tensor $\boldsymbol{b}$ is an element of a three-dimensional space. A usual basis of this space is made of the three tensors:

$$\begin{aligned}
\boldsymbol{T}_1 &= \boldsymbol{S} \\
\boldsymbol{T}_2 &= \boldsymbol{SW} - \boldsymbol{WS} \\
\boldsymbol{T}_3 &= \boldsymbol{S}^2 - \frac{1}{3}\{\boldsymbol{S}^2\}\boldsymbol{I}
\end{aligned} \qquad (6)$$

such that $\boldsymbol{b}$ can be written:

$$\boldsymbol{b} = \sum_{n=1}^{3} \alpha_n \boldsymbol{T}_n \qquad (7)$$

The Galerkin projection consists in introducing the decomposition (7) into Eq. (5) and projecting the equation on the basis tensor $\boldsymbol{T}_m$, which yields:

$$\begin{aligned}
\sum_{n=1}^{3}\alpha_n \Bigg[&-\frac{1}{a_4}\{\boldsymbol{T}_n\boldsymbol{T}_m\} - a_3(\{\boldsymbol{T}_n\boldsymbol{S}\boldsymbol{T}_m\} + \{\boldsymbol{S}\boldsymbol{T}_n\boldsymbol{T}_m\}) \\
&+a_2(\{\boldsymbol{T}_n\boldsymbol{W}\boldsymbol{T}_m\} - \{\boldsymbol{W}\boldsymbol{T}_n\boldsymbol{T}_m\}) \\
&-a_5\left(\{\boldsymbol{T}_n\boldsymbol{M}\boldsymbol{T}_m\} + \{\boldsymbol{M}\boldsymbol{T}_n\boldsymbol{T}_m\} - \frac{1}{2}\{\boldsymbol{bM}\}\{\boldsymbol{M}\boldsymbol{T}_m\}\right)\Bigg] \\
&= a_1\{\boldsymbol{S}\boldsymbol{T}_m\} + \frac{a_5}{2}\{\boldsymbol{M}\boldsymbol{T}_m\}
\end{aligned} \qquad (8)$$

Defining the invariants:

$$\begin{aligned}
\eta &= \sqrt{\{\boldsymbol{S}^2\}} \\
\mathcal{R} &= \sqrt{-\frac{\{\boldsymbol{W}^2\}}{\{\boldsymbol{S}^2\}}} \\
\mathcal{P} &= \{\boldsymbol{SM}\} \\
\mathcal{Q} &= 2\{\boldsymbol{SWM}\}
\end{aligned} \qquad (9)$$

the following matricial relation is obtained:

$$\boldsymbol{AX} = \boldsymbol{Y} \qquad (10)$$

where $X_i = \alpha_i$ and $\boldsymbol{A}$ is the 3×3 matrix:

$$\begin{bmatrix}
-\frac{\eta^2}{a_4} - \frac{a_5}{3}\eta^2 + \frac{a_5}{2}\mathcal{P}^2 & -2a_2\eta^4 R^2 + \frac{a_5}{2}\mathcal{P}\mathcal{Q} & -\frac{a_3}{3}\eta^4 - \frac{a_5}{4}\eta^2\mathcal{P} \\
2a_2\eta^4 R^2 + \frac{a_5}{2}\mathcal{P}\mathcal{Q} & -\frac{2}{a_4}\eta^4 R^2 - \frac{2}{3}a_5\eta^4 R^2 + \frac{a_5}{2}\mathcal{Q}^2 & -\frac{a_5}{4}\eta^2\mathcal{Q} \\
-\frac{a_3}{3}\eta^4 - \frac{a_5}{4}\eta^2\mathcal{P} & -\frac{a_5}{4}\eta^2\mathcal{Q} & -\frac{\eta^4}{6a_4} + \frac{5}{72}a_5\eta^4
\end{bmatrix} \qquad (11)$$

$\boldsymbol{Y}$ is given by:

$$\boldsymbol{Y} = \begin{bmatrix} a_1 \eta^2 + \frac{a_5}{2} \mathcal{P} \\ \frac{a_5}{2} \mathcal{Q} \\ \frac{a_5}{12} \eta^2 \end{bmatrix} \tag{12}$$

Again, it is worth pointing out that $\boldsymbol{A}$ and $\boldsymbol{Y}$ reduce to the ones found by Rumsey *et al.* (2000) when the blending function α goes to 1. Therefore, it is clear that the wall-blocking effect enters the problem through the variation with α of the coefficients a_i, which, in particular, turns on the terms in a_5 in Eq. (11) and Eq. (12). The main difference with Rumsey *et al.*'s (2000) model is thus the appearance of two new invariants, $\mathcal{P}$ and $\mathcal{Q}$. The model is thus dependent on 4 invariants, defined by Eq. (9), which represent different physical mechanisms:

- η simply characterizes the mean strain. It reduces to $\eta = \frac{1}{\sqrt{2}} \partial U / \partial y$ in a channel flow.
- $\mathcal{R}$ is merely the mean *kinematic vorticity number* of Truesdell (1953). It is a pointwise measurement of the "quality" of mean rotation: it is linked with $\mathrm{Q} = \frac{1}{2}(\|\boldsymbol{W}^2\| - \|\boldsymbol{S}^2\|)$, the second invariant of the mean velocity gradient (not to be confused with $\mathcal{Q} = 2\{\boldsymbol{SWM}\}$ used in the present paper), by the relation $\mathrm{Q} = \frac{1}{2}(\mathcal{R}^2 - 1)\eta^2$. Since Q is the first component of the mean pressure Laplacian (the second component being the mean contribution of the fluctuating field), $\mathcal{R} > 1$ identifies regions where the mean flow tends to reduce the mean pressure, which are the regions where the mean flow rotates. $\mathcal{R} = 0$ and $\mathcal{R} = 1$ correspond to plane strain and pure shear regions, respectively. Obviously, $\mathcal{R} = 1$ in a channel flow.
- $\mathcal{P} = \{\boldsymbol{SM}\}$ is a new invariant indicative of the relative orientation of the principal axes of the mean strain tensor and of the "wall-normal" tensor. It is defined everywhere in the domain and is sensitive to the presence of all solid boundaries. When a plane wall is approached, it goes to:

  $$\mathcal{P} = \frac{\partial U_\mathrm{n}}{\partial x_\mathrm{n}} \tag{13}$$

  where the subscript n denotes the wall-normal component (of course, no summation on n). $\mathcal{P}^2/\eta^2$ can be called *the impingement invariant*, since it reaches its maximum value $\mathcal{P}^2/\eta^2 = 2/3$ at axisymmetric impingement points (e.g., in the case of an axisymmetric jet impinging on a flat plate) and its minimum value $\mathcal{P}^2/\eta^2 = 0$ when the flow is parallel to the wall (e.g., in a channel flow).
- $\mathcal{Q} = 2\{\boldsymbol{SWM}\}$ is also a new invariant, which, similarly to $\mathcal{P}$, characterizes the orientation of the velocity gradients compared to the "wall normal" direction. Close to a plane wall, it reduces to

  $$\mathcal{Q} = \frac{1}{2}\left(\frac{\partial U_{\mathrm{t}_1}}{\partial x_\mathrm{n}}^2 - \frac{\partial U_\mathrm{n}}{\partial x_{\mathrm{t}_1}}^2 + \frac{\partial U_{\mathrm{t}_2}}{\partial x_\mathrm{n}}^2 - \frac{\partial U_\mathrm{n}}{\partial x_{\mathrm{t}_2}}^2\right) \tag{14}$$

  where n denotes again the wall-normal component, and t_1 and t_2 the two components tangential to the wall. Equation (14) shows that $\mathcal{Q}$ is high when the shear is oriented like in a developed boundary layer. $\mathcal{Q}$ is not sensitive to plane strain. Therefore, $\mathcal{Q}/\eta^2$, which is between -1 and 1, is an invariant that characterizes the resemblance of the local mean flow to a fully developed boundary layer. It can be called *the boundary layer invariant.* Using both $\mathcal{P}^2/\eta^2$ and $\mathcal{Q}/\eta^2$ helps the identification of the local flow structure in the vicinity of a wall, since their values are known for typical flow configurations above flat plates:

Boundary layer	$\mathcal{P}^2/\eta^2 \to 0$	$\mathcal{Q}/\eta^2 \to 1$
Channel flow	$\mathcal{P}^2/\eta^2 = 0$	$\mathcal{Q}/\eta^2 = 1$
Axisymmetric impingement point	$\mathcal{P}^2/\eta^2 = 2/3$	$\mathcal{Q}/\eta^2 = 0$
2D impingement point	$\mathcal{P}^2/\eta^2 = 1/2$	$\mathcal{Q}/\eta^2 = 0$

Thus, the selective influence of the blocking effect will be driven in the model by the values of $\mathcal{P}$ and $\mathcal{Q}$.

The projection coefficients α_n of the anisotropy tensor $\boldsymbol{b}$ are given by:

$$\boldsymbol{X} = \boldsymbol{A}^{-1}\boldsymbol{Y} \tag{15}$$

which can be easily evaluated by a symbolic calculator:

$$\begin{aligned}
\alpha_1 = -\frac{3 a_4 \eta^2}{\psi} \Big[& 3 a_4 a_5 \left(3 a_1 + (a_1 - 2 a_3) a_4 a_5\right) \mathcal{Q}^2 \\
& + 2 a_5 \left(-3 + 2 a_4 a_5\right) \left((3 + a_4 a_5) \mathcal{P} - 3 a_2 a_4 \mathcal{Q}\right) R^2 \eta^2 \\
& + \left(3 + a_4 a_5\right) \left(2 a_3 a_4 a_5 + a_1 (-12 + 5 a_4 a_5)\right) R^2 \eta^4 \Big]
\end{aligned}$$

$$\begin{aligned}
\alpha_2 = -\frac{3 a_4 \eta^2}{\psi} \Big[& a_5 \left(-9 + a_4 a_5 (3 + 2 a_4 a_5) - 3 a_4 \left(3 a_1 + (a_1 - 2 a_3) a_4 a_5\right) \mathcal{P}\right) \mathcal{Q} \\
& + 3 a_4 a_5 \left(a_3 (-3 a_1 + 2 a_3) a_4 \mathcal{Q} + 2 a_2 (-3 + 2 a_4 a_5) \mathcal{P} R^2\right) \eta^2 \\
& + 3 a_2 a_4 \left(2 a_3 a_4 a_5 + a_1 (-12 + 5 a_4 a_5)\right) R^2 \eta^4 \Big]
\end{aligned}$$

$$\begin{aligned}
\alpha_3 = \frac{6 a_4}{\psi} \Big[& -3 a_4 {a_5}^2 \left(3 + a_4 a_5\right) \mathcal{Q}^2 \\
& - 3 a_4 a_5 \left(-3 a_1 a_3 a_4 \mathcal{Q}^2 + 2 a_5 (3 + a_4 a_5) \mathcal{P}^2 R^2\right) \eta^2 \\
& + a_5 \left((3 + a_4 a_5) \left(3 + a_4 (a_5 - 3 (3 a_1 + 2 a_3) \mathcal{P})\right) - 9 a_2 (3 a_1 - 2 a_3) {a_4}^2 \mathcal{Q}\right) R^2 \eta^4 \\
& + 6 a_4 R^2 \left(-2 a_1 a_3 (3 + a_4 a_5) + 3 {a_2}^2 a_4 a_5 R^2\right) \eta^6 \Big]
\end{aligned}$$

$$\begin{aligned}
\psi = \; & 3 a_4 a_5 (3 + a_4 a_5)^2 Q^2 \eta^2 \\
& + 6 a_4 a_5 \left(-3 {a_3}^2 {a_4}^2 Q^2 + (3 + a_4 a_5)^2 P^2 R^2\right) \eta^4 \\
& + \left(3 + a_4 a_5\right) \left(-36 + a_4 a_5 (3 + 5 a_4 a_5 + 36 a_3 a_4 P)\right) R^2 \eta^6 \\
& + 6 {a_4}^2 R^2 \left(4 {a_3}^2 (3 + a_4 a_5) + 3 {a_2}^2 (-12 + 5 a_4 a_5) R^2\right) \eta^8
\end{aligned} \tag{16}$$

The residual nonlinearity of the model, quoted in the previous section, only appears in the equation for α_1, since a_4 is a function of α_1, through the ratio production/dissipation:

$$\frac{P}{\varepsilon} = -2\{\boldsymbol{bS}\}\tau = -2\alpha_1 \eta^2 \tau \tag{17}$$

It would be possible to consider the ratio P/ε as constant, similarly to what was done initially by Gatski and Speziale (1993), but further studies (Ying and Canuto, 1996; Girimaji, 1996; Jongen *et al.*, 1998) suggest that using Eq. (17) greatly improves the predictions.

Since in Eq. (16), the α_1 equation involves ${a_4}^3$, and a_4 is in ${\alpha_1}^{-1}$, this equation is quartic in α_1. Therefore, it is necessary to solve the following quartic algebraic expression for α_1:

$$\beta_4 \alpha_1^4 + \beta_3 \alpha_1^3 + \beta_2 \alpha_1^2 + \beta_1 \alpha_1 + \beta_0 = 0 \tag{18}$$

The coefficients β_n are given in the appendix.

The selection of the proper root for this equation is not an issue in the present paper, since only a channel flow will be computed: in that case, Eq. (7) reduces to:

$$b = \begin{bmatrix} -\alpha_2\eta^2 + \frac{\alpha_3}{6}\eta^2 & \frac{\alpha_1}{\sqrt{2}}\eta & 0 \\ \frac{\alpha_1}{\sqrt{2}}\eta & \alpha_2\eta^2 + \frac{\alpha_3}{6}\eta^2 & 0 \\ 0 & 0 & -\frac{\alpha_3}{3}\eta^2 \end{bmatrix} \quad (19)$$

Since $\eta = 1/\sqrt{2}\ \partial U/\partial y$, it is clear that $-k\alpha_1$ plays the role of an eddy-viscosity. Therefore, α_1 is expected to be negative. Now, a study (not given here) of the solutions of Eq. (18) at many different locations in a channel gave always the same picture: one solution is negative, one solution is positive and the two other solutions are complex. Therefore, Eq. (18) was simply solved by Newton's method initiated with the value $-0.09k/\varepsilon$, which always gave a negative solution.

Once the value of α_1 is known, α_2 and α_3 can be simply evaluated using Eq. (16). The anisotropy tensor $\boldsymbol{b}$ and, *ipso facto*, the Reynolds stresses are then obtained by Eq. (7).

This algebraic formulation is solved with 3 differential equations for k, ε and α (the elliptic blending function). The complete set of equations is given in the appendix. It is worth noting that, contrary to Rumsey *et al.*'s model, Durbin's (1993) form of the ε equation is used, which consists in bounding the turbulent time scale k/ε by the Kolmogorov time scale. Another difference to be pointed out concerns the turbulent diffusion terms in the transport equations for k and ε: while Rumsey *et al.* used an equilibrium eddy-viscosity $\nu_t = C_\mu k^2/\varepsilon$, the k–ε–α model uses the Daly–Harlow (1970) model (see the appendix). In a channel flow, the Daly–Harlow model is equivalent to an eddy-viscosity model in which $\nu_t = C_\mu \overline{v^2} k/\varepsilon$, which highlights some similarity between the present k–ε–α model and the $\overline{v^2}$–f model (Durbin, 1991). However, the k–ε–α model has many virtues compared to the $\overline{v^2}$–f model: it resolves all the anisotropies; it does not rely upon the controversial definition of the scalar "$\overline{v^2}$"; it derives from the SSG model, which is more elaborate than the Rotta+IP model used in the $\overline{v^2}$–f; the boundary condition for the function driving the blocking effect is simply $\alpha = 0$, to be compared to $f = -20\nu^2\overline{v^2}/\varepsilon y^4$, which is known for leading to numerical difficulties in the $\overline{v^2}$–f model.

LIMITING BEHAVIOR OF THE ANISOTROPIES

The different roles in a channel flow of the three projection coefficient clearly appear in Eq. (19). α_1, which is the weight of the tensor $\boldsymbol{S}$ in $\boldsymbol{b}$, only drives the shear stress. α_3 drives the spanwise anisotropy and α_2 differentiates b_{22} from b_{11}.

In the vicinity of the wall, a study (not given here) of the limiting form of Eq. (18) shows that the only solution at the wall is $\alpha_1 = 0$.

Similarly, it is easy to show that $\alpha_2 \to -1/(4\eta^2)$ and $\alpha_3 \to -1/(2\eta^2)$. These values of the coefficients lead to the limiting form of the anisotropy tensor in the vicinity of the wall:

$$b = \alpha_1\frac{\eta}{\sqrt{2}}\begin{bmatrix} 0 & 1 & 0 \\ 1 & 0 & 0 \\ 0 & 0 & 0 \end{bmatrix} + \alpha_2\eta^2\begin{bmatrix} -1 & 0 & 0 \\ 0 & 1 & 0 \\ 0 & 0 & 0 \end{bmatrix} + \alpha_3\frac{\eta^2}{12}\begin{bmatrix} 1 & 0 & 0 \\ 0 & 1 & 0 \\ 0 & 0 & -2 \end{bmatrix}$$
$$= \begin{bmatrix} 1/6 & 0 & 0 \\ 0 & -1/3 & 0 \\ 0 & 0 & 1/6 \end{bmatrix} \quad (20)$$

The crucial two-component limit of turbulence is thus reproduced, since Eq. (20) shows that $\overline{v^2} \ll \overline{u^2}$ and $\overline{v^2} \ll \overline{w^2}$. Note that DNS in a channel does not give $b_{11} = b_{33}$, but this feature of the model allows the reproduction of the rapid change of b_{11} and b_{33} in the vicinity of the wall shown in Fig. 1a.

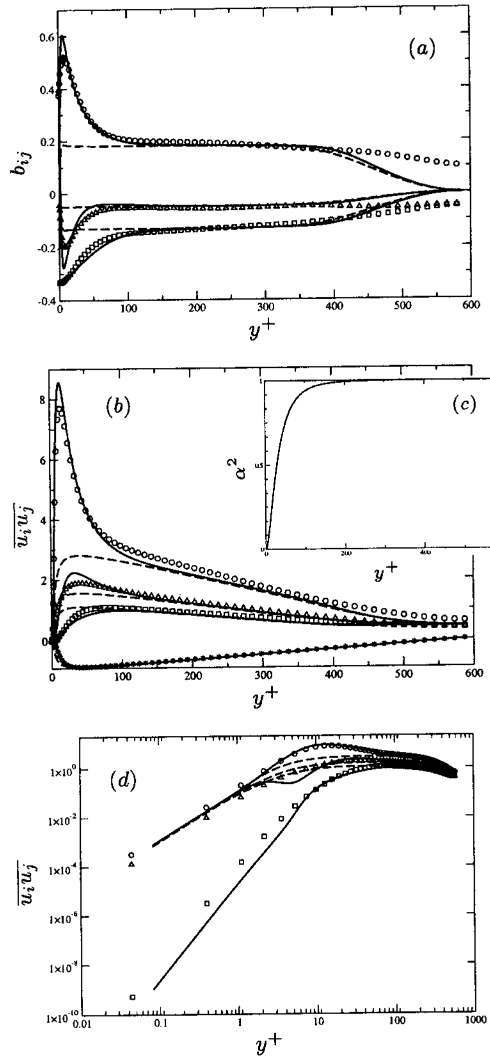

Figure 1: Comparison of the k–ε–α model with the model of Rumsey *et al.* (2000). Symbols: DNS at $Re_\tau = 590$ (Moser *et al.*, 1999); ——— Rumsey *et al.* model; ——— k–ε–α model. (a) Anisotropies; (b) Reynolds stresses; (c) Blending function α^2 (d) Reynolds stresses in log–log scale. (○ 11–component; □ 22–component; △ 33–component; ∗ 12–component).

CHANNEL FLOW RESULTS

Fig. 1 shows the predictions of the k–ε–α model compared to the model of Rumsey *et al.* (2000), which is the same model without the blocking effect of the wall. It is clear that, far from the wall, the two models give the same solution. The interest of introducing the blocking effect of the wall appears in Fig. 1: the SSG model, and consequently its algebraic version, is indeed able to reproduce correctly the anisotropies in the upper part of the log layer, but not their rapid variations below $y^+ = 100$, which are due to the kinematic blocking of the wall. This effect is driven in the k–ε–α model by the value of the blending function α^2, shown in Fig. 1c. In the vicinity of the wall, $\alpha \to 0$, which forces the anisotropy to the limiting form (20): it is seen in Fig. 1a that the wall-normal component of the anisotropy tensor indeed goes to $-1/3$ at the wall, which is the signature of

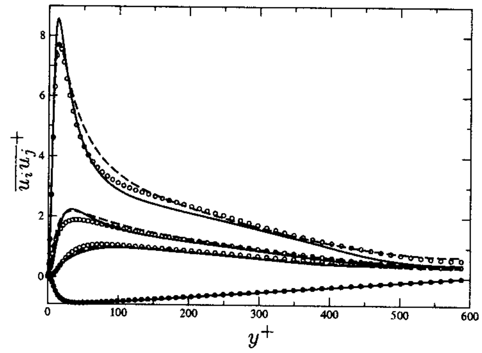

Figure 2: Comparison of the k–ε–α model (3 equations) with its underlying Reynolds stress model (Elliptic Blending Model, 8 equations). Symbols: DNS at $Re_\tau = 590$ (Moser *et al.*, 1999) (○ $\overline{u^2}$; □ $\overline{v^2}$; △ $\overline{w^2}$; ∗ $\overline{uv}$.) ; ––– EBM; —— k–ε–α model.

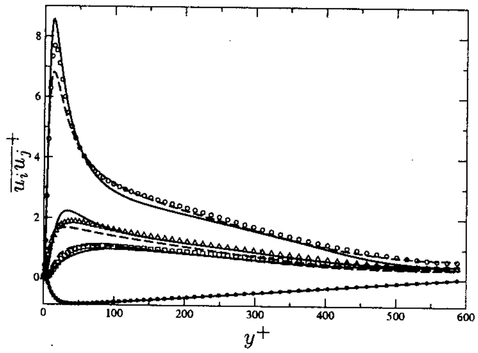

Figure 3: Comparison between the full Reynolds stress model of Durbin (1993) (13 equations) and the k–ε–α model (3 equations). Symbols: DNS at $Re_\tau = 590$ (Moser *et al.*, 1999) (○ $\overline{u^2}$; □ $\overline{v^2}$; △ $\overline{w^2}$; ∗ $\overline{uv}$.) ––– Durbin's model. —— k–ε–α model.

the two-component limit of turbulence. Moreover, $\overline{v^2}$ is not only negligible compared to $\overline{u^2}$ and $\overline{w^2}$: it is seen in Fig. 1d that the limiting behaviour $\overline{v^2} = \mathcal{O}(y^4)$ is obtained, which validates the correct reproduction of the wall-blocking.

Fig. 2 shows a comparison between the k–ε–α model and its underlying Reynolds-stress model, the Elliptic Blending Model (EBM). The predicted Reynolds stresses are very similar, which shows that the explicit algebraic methodology is almost "non intrusive" in the case of a channel flow. Indeed, during the derivation of the model, the only hypothesis that was used and is not strictly valid in a channel flow is Eq. (2). The main consequence is the wrong prediction of the anisotropy in the centre of the channel: indeed, when the mean velocity gradient approaches zero, the diffusion terms become dominant in the budgets of the Reynolds stresses and do not conform to Eq. (2). Relating diffusion to the anisotropy tensor $\boldsymbol{b}$ leads to a fully linear model when $P \to 0$. Therefore, at the centre of the channel, Eq. (3) reduces to a balance between slow redistribution and dissipation: $-g_1 \boldsymbol{b}/2\tau + \boldsymbol{b}/\tau = 0$: the only solution to this equation is of course $b_{ij} = 0$. Note that using the nonlinear slow term of the original SSG model (g_2 term) would lead to the same result.

Fig. 3 illustrates the interest of the present approach. Durbin's (1993) model (rescaled version of Manceau *et al.*, 2002), consists of 13 closure equations: 1 for the dissipation rate, 6 for the Reynolds stresses and 6 elliptic relaxation equations. By reducing the number of elliptic relaxation equations to 1 (Elliptic Blending Model) and applying the explicit algebraic methodology, the number of differential equations is reduced to 3 (k–ε–α). Fig. 3 shows that the reproduction of the near-wall anisotropy is not spoiled.

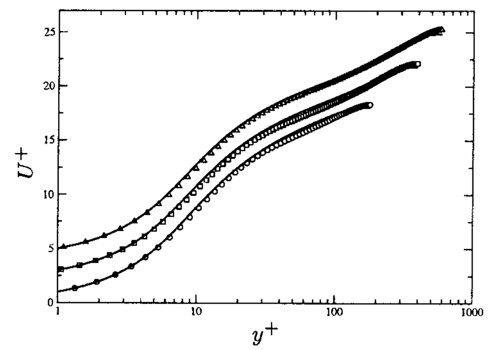

Figure 4: Mean velocity profiles predicted by the k–ε–α model at different Reynolds numbers. Symbols: DNS (Moser *et al.*, 1999) at ○ $Re_\tau = 180$, □ $Re_\tau = 395$, △ $Re_\tau = 590$; —— k–ε–α model.

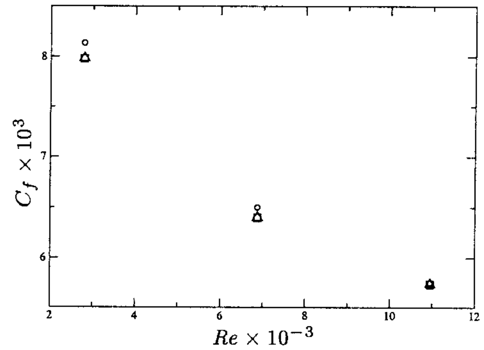

Figure 5: Variation of the friction coefficient C_f with Reynolds number. ○ DNS (Moser *et al.*, 1999); □ Elliptic Blending Model; △ k–ε–α model.

Fig. 4 shows the excellent predictions of the mean velocity profiles at different Reynolds numbers. Consequently, the variation of the friction coefficient C_f with the Reynolds number, shown in Fig. 5, is very well reproduced. The results shown in Figs. 3, 4 and 5 are of considerable interest in the frame of industrial applications for which the computational cost, but also the reproduction of the physics, are crucial issues.

CONCLUSION

The theoretical analyses and the channel flow results given in this paper are very encouraging for the ability of the new Explicit Algebraic Stress Model, the k–ε–α model, to reproduce the turbulence anisotropy is more complex configurations. Indeed, the underlying redistribution model (SSG) is known for giving satisfactory results in many situations and Rumsey *et al.* (2000) showed that the explicit algebraic version of the SSG (with a variable P/ε), is able to reproduce the flow in a strongly curved U-duct. The present work is an extension of their work in order to account for the blocking effect of the wall: the new model was shown to reproduce the two-component limit of turbulence in a channel flow. The methodology, based on elliptic blending and tensorial representation, is valid for any 2D flow. The appearance in the near-wall region of terms involving invariants ($\mathcal{P}$ and $\mathcal{Q}$) sensitive to the orientation of the mean velocity gradient with respect to the wall indicates that the model is not only suited to particular flow configurations: the kinematic blocking of the wall will adapt itself to the situation and is expected to modify the redistribution processes such a way that the two-component limit of turbulence is always reached at the wall. While theoretical and numerical results show that it is indeed the case in a channel flow, further work is needed to confirm this favourable behaviour in other configurations. In particular, the use of a three-term basis and simplifications of the invariants using a 2D hypothesis will require some precautions in order to apply the model to 3D configurations.

ACKNOWLEDGEMENTS

This work was initiated during a stay at NASA Langley Research Center. The author is grateful to NASA for its hospitality and in particular to Tom Gatski for his kindness and for many useful discussions.

APPENDIX

Linearized Elliptic Blending Model:

$$\phi_{ij} = (1-\alpha^2)\,\phi^w_{ij} + \alpha^2\phi^h_{ij} \tag{21}$$

$$\varepsilon_{ij} = (1-\alpha^2)\frac{\overline{u_i u_j}}{k}\varepsilon + \frac{2}{3}\alpha^2\varepsilon\delta_{ij} \tag{22}$$

$$\begin{aligned}\phi^h_{ij} = &-\left(g_1 + g_1^*\frac{P}{\varepsilon}\right)\varepsilon b_{ij} + \left(g_3 - g_3^*\sqrt{1-\alpha^2}\right)kS_{ij}\\ &+g_4 k\left(b_{ik}S_{jk} + b_{jk}S_{ik} - \frac{2}{3}b_{lm}S_{lm}\delta_{ij}\right)\\ &+g_5 k\,(b_{ik}W_{jk} + b_{jk}W_{ik})\end{aligned} \tag{23}$$

$$\phi^w_{ij} = -5\frac{\varepsilon}{k}\left[\tau_{ik}n_j n_k + \tau_{jk}n_i n_k - \frac{1}{2}\tau_{kl}n_k n_l\,(n_i n_j + \delta_{ij})\right] \tag{24}$$

New Explicit Algebraic Stress Model (k–ε–α):

$$\frac{\mathrm{D}k}{\mathrm{D}t} = P - \varepsilon + \frac{\partial}{\partial x_k}\left(\frac{C_\mu}{\sigma_k}\tau_{kl}\,T\frac{\partial k}{\partial x_l}\right) + \nu\frac{\partial^2 k}{\partial x_k \partial x_k} \tag{25}$$

$$\frac{\mathrm{D}\varepsilon}{\mathrm{D}t} = \frac{C'_{\varepsilon_1}P - C_{\varepsilon_2}\varepsilon}{T} + \frac{\partial}{\partial x_k}\left(\frac{C_\mu}{\sigma_\varepsilon}\tau_{kl}\,T\frac{\partial \varepsilon}{\partial x_l}\right) + \nu\frac{\partial^2 \varepsilon}{\partial x_k \partial x_k} \tag{26}$$

$$\alpha - L^2\nabla^2\alpha = 1 \tag{27}$$

$$\text{Wall BC:}\quad k = 0 \quad ; \quad \varepsilon = 2\nu\frac{k}{y^2} \quad ; \quad \alpha = 0 \tag{28}$$

$$\tau_{ij} = 2k(b_{ij} + 1/3\delta_{ij}) \tag{29}$$

$$\boldsymbol{n} = \boldsymbol{\nabla}\alpha/\|\boldsymbol{\nabla}\alpha\| \tag{30}$$

$$\boldsymbol{b} = \alpha_1\boldsymbol{S} + \alpha_2\,(\boldsymbol{SW} - \boldsymbol{WS}) + \alpha_3\left(\boldsymbol{S}^2 - \frac{1}{3}\{\boldsymbol{S}^2\}\boldsymbol{I}\right) \tag{31}$$

α_1: see Eqs. (34) and (35); α_2 and α_3: see Eq. (16)

$$C'_{\varepsilon_1} = C_{\varepsilon_1}\left(1. + A_1\left(1-\alpha^2\right)\sqrt{\frac{k}{\tau_{ij}n_i n_j}}\right) \tag{32}$$

$$\begin{gathered}C_{\varepsilon_1} = 1.44\,;\; C_{\varepsilon_2} = 1.85\,;\; A_1 = 0.02\,;\; \sigma_\varepsilon = 1.15\,;\\ \sigma_k = 1.0\,;\; C_L = 0.161\,;\; C_\eta = 80.0\,;\; C_T = 6.0\,;\\ g_1 = 3.4\,;\; g_1^* = 1.8\,;\; g_3 = 0.4\,;\; g_3^* = 0.4\,;\; g_4 = 1.25\,;\; g_5 = 0.4\end{gathered} \tag{33}$$

$$\beta_4\alpha_1^4 + \beta_3\alpha_1^3 + \beta_2\alpha_1^2 + \beta_1\alpha_1 + \beta_0 = 0 \tag{34}$$

$$\begin{aligned}
\beta_0 = 3\,\tau\,\Big[&3\,a_5\,\mathcal{Q}^2\,\tau\,(3\,a_1\,\gamma_1 + a_1\,a_5\,\tau - 2\,a_3\,a_5\,\tau)\\
&+\mathcal{R}^2\,\eta^2\,\Big[-36\,a_1\,\gamma_1{}^2\,\eta^2 + 4\,a_5{}^3\,\mathcal{P}\,\tau^2\\
&+3\,a_5\,\gamma_1\,\Big(-6\,\mathcal{P}\,\gamma_1 + \Big(6\,a_2\,\mathcal{Q} + (a_1 + 2\,a_3)\,\eta^2\Big)\,\tau\Big)\\
&+a_5{}^2\,\tau\,\Big(6\,\mathcal{P}\,\gamma_1 + \Big(-12\,a_2\,\mathcal{Q} + (5\,a_1 + 2\,a_3)\,\eta^2\Big)\,\tau\Big)\Big]\Big]\\
\beta_1 = 18\,&a_2{}^2\,\mathcal{R}^4\,\eta^6\,\tau^2\,(-12\,\gamma_1 + 5\,a_5\,\tau)\\
&+3\,a_5\,\mathcal{Q}^2\,\tau\,\Big[9\,\gamma_1{}^2 + 6\,a_5\,\gamma_1\,\tau + \Big(a_5{}^2 - 6\,\Big(a_3{}^2 + 3\,a_1\,\gamma_0\Big)\,\eta^2\Big)\,\tau^2\Big]\\
&+\mathcal{R}^2\,\eta^2\,\Big[-108\,\gamma_1{}^3\,\eta^2 + 27\,a_5\,\gamma_1{}^2\,\Big(2\,\mathcal{P}^2 - \eta^2\Big)\,\tau\\
&+18\,\gamma_1\,\Big(6\,a_5\,\mathcal{P}\,(a_3 + 2\,\gamma_0)\,\eta^2 + 4\,\Big(a_3{}^2 + 6\,a_1\,\gamma_0\Big)\,\eta^4 + a_5{}^2\,\Big(2\,\mathcal{P}^2 + \eta^2\Big)\Big)\,\tau^2\\
&+a_5\,\Big[36\,a_5\,\mathcal{P}\,(a_3 - \gamma_0)\,\eta^2 + a_5{}^2\,\Big(6\,\mathcal{P}^2 + 5\,\eta^2\Big)\\
&-6\,\Big(18\,a_2\,\mathcal{Q}\,\gamma_0\,\eta^2 + \Big(-4\,a_3{}^2 + 3\,a_1\,\gamma_0 + 6\,a_3\,\gamma_0\Big)\,\eta^4\Big)\Big]\,\tau^3\Big]\\
\beta_2 = 18\,&a_2{}^2\,\mathcal{R}^4\,\eta^6\,\tau^2\,(-12\,\gamma_1 + 5\,a_5\,\tau) + 3\,a_5\,\mathcal{Q}^2\,\tau\,\Big[9\,\gamma_1{}^2 + 6\,a_5\,\gamma_1\,\tau\\
&+\Big(a_5{}^2 - 6\,\Big(a_3{}^2 + 3\,a_1\,\gamma_0\Big)\,\eta^2\Big)\,\tau^2\Big] + \mathcal{R}^2\,\eta^2\,\Big[-108\,\gamma_1{}^3\,\eta^2\\
&+27\,a_5\,\gamma_1{}^2\,\Big(2\,\mathcal{P}^2 - \eta^2\Big)\,\tau + 18\,\gamma_1\,\Big(6\,a_5\,\mathcal{P}\,(a_3 + 2\,\gamma_0)\,\eta^2\\
&+4\,\Big(a_3{}^2 + 6\,a_1\,\gamma_0\Big)\,\eta^4 + a_5{}^2\,\Big(2\,\mathcal{P}^2 + \eta^2\Big)\Big)\,\tau^2 + a_5\,\Big[36\,a_5\,\mathcal{P}\,(a_3 - \gamma_0)\,\eta^2\\
&+a_5{}^2\,\Big(6\,\mathcal{P}^2 + 5\,\eta^2\Big) - 6\,\Big(18\,a_2\,\mathcal{Q}\,\gamma_0\,\eta^2 + \Big(-4\,a_3{}^2 + 3\,a_1\,\gamma_0 + 6\,a_3\,\gamma_0\Big)\,\eta^4\Big)\Big]\,\tau^3\Big]\\
\beta_3 = 108\,&\gamma_0{}^2\,\eta^4\,\tau^2\,\Big[a_5\,\mathcal{Q}^2\,\tau - \mathcal{R}^2\,\Big(12\,\gamma_1\,\eta^4 + a_5\,\eta^2\,\Big(-2\,\mathcal{P}^2 + \eta^2\Big)\,\tau\Big)\Big]\\
\beta_4 = 864\,&\mathcal{R}^2\,\gamma_0{}^3\,\eta^{10}\,\tau^3
\end{aligned} \tag{35}$$

REFERENCES

T. J. Craft and B. E. Launder, 1996, "A Reynolds stress closure designed for complex geometries", *Intl J. Heat and Fluid Flow*, 17(3):245–254.

B. J. Daly and F. H. Harlow, 1970, "Transport equations in turbulence", *Phys. Fluids*, 13:2634–2649.

P. A. Durbin, 1991, "Near-wall turbulence closure modeling without 'damping functions'", *Theoret. Comput. Fluid Dynamics*, 3:1–13.

P. A. Durbin, 1993, "A Reynolds stress model for near-wall turbulence", *J. Fluid Mech.*, 249:465–498.

T. B. Gatski and C. G. Speziale, 1993, "On explicit algebraic stress models for complex turbulent flows", *J. Fluid Mech.*, 254:59–78.

S. S. Girimaji, 1996, "Fully explicit and self-consistent algebraic Reynolds stress model", *Theoret. Comp. Fluid Dynamics*, 8:387–402.

T. Jongen, L. Machiels, and T. B. Gatski, 1998, "Predicting noninertial effects with linear and nonlinear eddy-viscosity and algebraic stress models", *Flow, Turb. and Comb.*, 60:215–234.

R. Manceau, J. R. Carlson, and T. B. Gatski, 2002, "A rescaled elliptic relaxation approach: neutralizing the effect on the log layer", *Phys. Fluids*, 14(11):3868-3879.

R. Manceau and K. Hanjalić, 2002, "Elliptic blending model: A new near-wall Reynolds-stress turbulence closure", *Phys. Fluids*, 14(2):744–754.

R. D. Moser, J. Kim, and N. N. Mansour, 1999, "Direct numerical simulation of turbulent channel flow up to $Re_\tau = 590$", *Phys. Fluids*, 11(4):943–945.

S. B. Pope, 1975, "A more general effective viscosity hypothesis", *J. Fluid Mech.*, 72:331–340.

W. Rodi, 1976, "A new algebraic relation for calculating the Reynolds stresses", *Z. Angew. Math. Mech.*, 56:219–221.

C. L. Rumsey, T. B. Gatski, and J. H. Morrison, 2000, "Turbulence model predictions of strongly curved flow in a U-duct", *AIAA J.*, 38(8):1394–1402.

C. G. Speziale, S. Sarkar, and T. B. Gatski, 1991, "Modeling the pressure-strain correlation of turbulence: an invariant dynamical system approach", *J. Fluid Mech.*, 227:245–272.

L. Thielen, K. Hanjalić, R. Manceau, and H. Jonker, 2001, "Turbulence modelling in a single normally impinging jet", *Proc. ASME-PVP Conference, Atlanta, USA*.

C. Truesdell, 1953, *The kinematics of vorticity*, Indiana Unversity.

R. Ying and V. M. Canuto, 1996, "Turbulence modelling over two-dimensional hills using an algebraic Reynolds stress expression", *Boundary-Layer Meteorology*, 77:69–99.